Confronting dark energy models using galaxy cluster number counts

S. Basilakos[*]

Academy of Athens, Research Center for Astronomy and Applied Mathematics, Soranou Efesiou 4, 11527, Athens, Greece

M. Plionis[†]

Institute of Astronomy and Astrophysics, National Observatory of Athens, Thessio 11810, Athens, Greece,
and Instituto Nacional de Astrofísica, Óptica y Electrónica, 72000 Puebla, Mexico

J. A. S. Lima[‡]

Departamento de Astronomia (IAGUSP), Universidade de São Paulo, Rua do Matão, 1226, 05508-900, S. Paulo, Brazil

The mass function of cluster-size halos and their redshift distribution are computed for 12 distinct accelerating cosmological scenarios and confronted to the predictions of the conventional flat ΛCDM model. The comparison with ΛCDM is performed by a two-step process. First, we determine the free parameters of all models through a joint analysis involving the latest cosmological data, using supernovae type Ia, the cosmic microwave background shift parameter, and baryon acoustic oscillations. Apart from a braneworld inspired cosmology, it is found that the derived Hubble relation of the remaining models reproduces the ΛCDM results approximately with the same degree of statistical confidence. Second, in order to attempt to distinguish the different dark energy models from the expectations of ΛCDM, we analyze the predicted cluster-size halo redshift distribution on the basis of two future cluster surveys: (i) an X-ray survey based on the eROSITA satellite, and (ii) a Sunayev-Zeldovich survey based on the South Pole Telescope. As a result, we find that the predictions of 8 out of 12 dark energy models can be clearly distinguished from the ΛCDM cosmology, while the predictions of 4 models are statistically equivalent to those of the ΛCDM model, as far as the expected cluster mass function and redshift distribution are concerned. The present analysis suggests that such a technique appears to be very competitive to independent tests probing the late time evolution of the Universe and the associated dark energy effects.

I. INTRODUCTION

Recent studies in observational cosmology lead to the conclusion that the available high quality cosmological data, from supernovae type Ia (SNe Ia), matter power-spectrum analysis, the angular power spectrum of the cosmic microwave background (CMB), baryon acoustic oscillations (BAO), and other complementary probes, like the existence of old galaxies at high redshifts, are well fitted by an emerging "standard cosmological model" (see [1–8] and references therein). By assuming flatness, as theoretically required by inflation and the CMB observations, the standard model is described by the Friedmann equation,

$$H^2(a) = \left(\frac{\dot{a}}{a}\right)^2 = \frac{8\pi G}{3}[\rho_m(a) + \rho_{DE}(a)], \qquad (1.1)$$

where $a(t)$ is the scale factor of the Universe, $\rho_m(a)$ is the density corresponding to the sum of baryonic plus cold dark matter (the latter needed to explain clustering), and an extra component $\rho_{DE}(a)$, with negative pressure called

dark energy (DE, hereafter), that accelerates the cosmic expansion (for reviews see [9]).

Nowadays, the physics of dark energy is considered one of the most fundamental and challenging problems on the interface uniting astronomy, cosmology, and particle physics. In the last decade there have been theoretical debates among the cosmologists regarding the nature of this exotic component. Many candidates have been proposed in the literature, such as a cosmological constant Λ (vacuum), time-varying Λ(t) cosmologies, quintessence, k-essence, quartessence, vector fields, phantom dark energy, tachyons, modifications of gravity, Chaplygin gas, and the list goes on (see [10–26] and references therein). Generically, some high energy field theories also suggest that the equation of state of such a dark energy is a function of cosmic time (see, for instance, [27]). Naturally, in order to establish the evolution of its equation of state (EOS), a realistic form of $H(a)$ is required and must be constrained through a combination of independent DE probes.

On the other hand, the abundance of collapsed structures as a function of mass and redshift is a key statistical test for studies of matter distribution in the Universe and, more importantly, it can readily be accessed from observations [28]. Indeed, the mass function of galaxy clusters has been measured based on X-ray surveys [29–31], via weak and

[*]svasil@academyofathens.noa.gr
[†]mplionis@astro.noa.gr
[‡]limajas@astro.iag.usp.br

strong lensing studies [32–34], using optical surveys, like the Sloan Digital Sky Survey (SDSS) [35,36], as well as, through the Sunayev-Zeldovich (SZ) effect [37]. In the last decade many authors have been involved in these kinds of studies and have found that the abundance of the collapsed structures is affected by the presence of a dark energy component [38–46].

In this work, we discuss how to differentiate a large family of flat DE cosmologies (12 models) from the conventional ΛCDM model. Initially, a joint statistical analysis, involving the latest observational data from SNe type Ia, CMB shift parameter, and BAO, is implemented. Since however the resulting Hubble functions of these DE models (apart a braneworld scenario) are statistically indistinguishable, we attempt to discriminate the different DE models by computing the halo mass function and the corresponding redshift distribution of the cluster-size halos. Finally, by using future X-ray and SZ surveys we show that the evolution of the cluster abundances (especially at large redshifts $z \gtrsim 0.5$), is a potential discriminator (in the Popper sense) for a large fraction of the studied DE models. As an extra bonus, we find that many of the DE models could be differentiated, from ΛCDM, even with the present available observational data from the galaxy cluster mass function.

The article is planned as follows. Section II provides the dark energy issue and the overall approach adopted in the paper. In Sec. III, a joint statistical analysis based on SNe Ia, CMB, and BAO is carried out for the conventional ΛCDM model. This statistical approach is used to constrain the DE model parameters and it is presented in Sec. IV. The linear growth factor of all models is discussed in Sec. V, while in Sec. VI, we discuss and compare the corresponding theoretical predictions regarding the evolution of the cluster abundances. Finally, the main conclusions are summarized in Sec. VII. Throughout the paper we adopt $H_0 = 71$ km/ sec /Mpc.

II. DARK ENERGY EQUATION OF STATE

In what follows, it will be assumed that the Universe is a self-gravitating fluid described by general relativity, and endowed with a spatially flat homogeneous and isotropic geometry. In addition, we also consider that it is filled by nonrelativistic matter plus a DE component (or some effective mechanism that simulates it), and whose equation of state, $p_{\rm DE} = w(a)\rho_{\rm DE}$, is driving the present accelerating stage. Following standard lines, the Hubble parameter reads

$$E^2(a) = \frac{H^2(a)}{H_0^2} = \Omega_m a^{-3} + \Omega_{\rm DE} e^{3 \int_a^1 d \ln y[1+w(y)]}, \quad (2.1)$$

where $E(a)$ is the normalized Hubble flow, Ω_m is the dimensionless matter density at the present epoch, $\Omega_{\rm DE} = 1 - \Omega_m$ denotes the DE density parameter, and $w(a)$ its EOS parameter. On the other hand, we can express the EOS

parameter in terms of $E(a) = H(a)/H_0$ [47] using the Friedmann equations as

$$w(a) = \frac{-1 - \frac{2}{3} a \frac{d \ln E}{da}}{1 - \Omega_m a^{-3} E^{-2}(a)}. \quad (2.2)$$

Since the exact nature of the DE has yet to be found, the above DE EOS parameter encodes our ignorance regarding the physical mechanism powering the late time cosmic acceleration.

The methodology described above can also be applied to the framework of modified gravity (see [23,48]). In this case, instead of using the exact Hubble flow through a modification of the Friedmann equation one may consider an equivalent Hubble flow somewhat mimicking Eq. (1.1). The key point here is that the accelerating expansion can be attributed to a kind of ''geometrical'' DE contribution. Now, since the matter density (baryonic + dark) cannot accelerate the cosmic expansion, we perform the following parametrization [23,48]:

$$E^2(a) = \frac{H^2(a)}{H_0^2} = \Omega_m a^{-3} + \delta H^2. \quad (2.3)$$

Naturally, any modification to the Friedmann equation of general relativity may be included in the last term of the above expression. After some algebra one may also derive, using Eqs. (2.2) and (2.3), an effective (geometrical) dark energy EOS parameter, given by

$$w(a) = -1 - \frac{1}{3} \frac{d \ln \delta H^2}{d \ln a}. \quad (2.4)$$

The above formulation will be adopted in our statistical analysis of all DE models discussed in Sec. IV.

III. LIKELIHOOD ANALYSIS: THE ΛCDM CASE

In this section we briefly present the basic observational samples and statistical analysis tools that will be used to constrain the cosmological parameters of the DE models. Here we discuss the ΛCDM model since it is now widely believed that if a better cosmology is called for, it will describe a cosmos that looks much like a ΛCDM model.

(i) Supernovas. In our statistical analysis we consider the *Constitution* set, containing 397 SNe type Ia, as compiled by Hicken *et al.* [6]. In order to avoid possible problems related to the local bulk flow, we use a subset of this sample containing 366 SNe Ia all with redshifts $z > 0.02$. The likelihood estimator is determined by a $\chi^2_{\rm SNIa}$ statistics

$$\chi^2_{\rm SNIa}(\mathbf{p}) = \sum_{i=1}^{366} \left[\frac{\mu^{\rm th}(a_i, \mathbf{p}) - \mu^{\rm obs}(a_i)}{\sigma_i} \right]^2, \quad (3.1)$$

where $a_i = (1 + z_i)^{-1}$ is the scale factor of the Universe in the observed redshift z_i, μ is the distance modulus $\mu = m - M = 5 \log d_L + 25$, and $d_L(a, \mathbf{p})$ is the luminosity distance, $d_L(a, \mathbf{p}) = ca^{-1} \int_a^1 \frac{dy}{y^2 H(y)}$.

(ii) Baryon acoustic oscillations (BAO). In addition to the SNe Ia data, we also consider the BAO scale produced in the last scattering surface by the competition between the pressure of the coupled baryon-photon fluid and gravity. The resulting acoustic waves leave (in the course of the evolution) an overdensity signature at certain length scales of the matter distribution. Evidence of this excess was recently found in the clustering properties of the SDSS galaxies [49], and it provides a suitable "standard ruler" for constraining DE models. In particular, we consider the following estimator:

$$A(\mathbf{p}) = \frac{\sqrt{\Omega_m}}{[z_s^2 E(a_s)]^{1/3}} \left[\int_{a_s}^1 \frac{da}{a^2 E(a)} \right]^{2/3},$$

measured from the SDSS data to be $A = 0.469 \pm 0.017$, where $z_s = 0.35$ [or $a_s = (1 + z_s)^{-1} \simeq 0.75$]. Therefore, the corresponding χ_{BAO}^2 function can be written as

$$\chi_{\text{BAO}}^2(\mathbf{p}) = \frac{[A(\mathbf{p}) - 0.469]^2}{0.017^2}, \qquad (3.2)$$

where $\mathbf{p}$ is a vector containing the cosmological fitting parameters.

(iii) CMB shift parameter. Another interesting geometrical probe for dark energy is provided by the angular scale of the sound horizon at the last scattering surface. It is encoded in the location l_1^{TT} of the first peak of the angular (CMB) power spectrum [50,51], and may be defined by the quantity $\mathcal{R} = \sqrt{\Omega_m} \int_{a_{ls}}^1 \frac{da}{a^2 E(a)}$. The shift parameter measured from the WMAP 7-year data [5] is $\mathcal{R} = 1.726 \pm 0.019$ at $z_{ls} = 1091.36$ [or $a_{ls} = (1 + z_{ls})^{-1} \simeq 9.154 \times 10^{-4}$]. In this case, the χ_{cmb}^2 function reads

$$\chi_{\text{cmb}}^2(\mathbf{p}) = \frac{[R(\mathbf{p}) - 1.726]^2}{0.019^2}. \qquad (3.3)$$

It should be stressed that for the CMB shift parameter, the contribution of the radiative component ($\Omega_R a^{-4}$, where $\Omega_R \simeq 4.174 \times 10^{-5} h^{-2}$) needs also to be considered [5]. Note also that the measured CMB shift parameter is somewhat model-dependent but mostly to models which are not included in our analysis. For example, such is the case when massive neutrinos are included or when there is a strongly time-varying equation of state parameter. The robustness of the shift parameter has been tested and discussed in [52].

In order to put tighter constraints on the corresponding parameter space of each DE model, the probes described above must be combined through a joint likelihood analysis,[1] given by the product of the individual likelihoods according to: $\mathcal{L}_{\text{tot}}(\mathbf{p}) = \mathcal{L}_{\text{SNIa}} \times \mathcal{L}_{\text{BAO}} \times \mathcal{L}_{\text{cmb}}$, which

translates in the joint χ^2 function in an addition: $\chi_{\text{tot}}^2(\mathbf{p}) = \chi_{\text{SNIa}}^2 + \chi_{\text{BAO}}^2 + \chi_{\text{cmb}}^2$. The results of this analysis provide $\Omega_m = 0.28 \pm 0.01$ with $\chi_{\text{tot}}^2(\Omega_m)/\text{dof} \simeq 439.6/367$.

In this concern, it should be remarked that a value of $\chi_{\text{SNIa}}^2 \simeq 439$ is what one gets by using directly the *Constitution* SNe Ia set of Hicken *et al.* [6] since the number of the SNe Ia used (366) dominates the overall χ_{tot}^2 budget of the joint likelihood. In addition, the corresponding goodness of fit ($\chi_{\text{SNIa}}^2/\text{dof} \simeq 1.2$) is significantly larger than the one found by Davis *et al.* [2] ($\chi_{\text{SNIa}}^2/\text{dof} \simeq 1$) from a previous sample containing 192 SNe Ia (see the discussion in [53,54]). Such a discrepancy appears to be the outcome of the different approaches chosen in order to join the different contributing SNe Ia sets. According to Hicken [55], in the case of the Davis *et al.* [2] data the nearby SNe Ia were imposed to provide $\chi^2/\text{dof} \simeq 1$ by hand, while no such fine-tuning was imposed on the *Constitution* set. Also the latter set includes distant SNe Ia which have typically larger distance modulus uncertainties with respect to those used in the Davis *et al.* sample [2]. In particular, this means that the higher $\chi_{\text{SNIa}}^2/\text{dof}$ value of the *Constitution* set should probably be attributed to typically lower SNe Ia distance modulus uncertainties.[2]

By using the most recent BAO results of Percival *et al.* [56], we have checked and verified that the above constraints of the flat ΛCDM model are not appreciably modified. Therefore, the reader should keep in mind the value $\chi_{\text{tot}}^2 \simeq 439.6$ for any further comparison with results predicted by the alternative DE models.

IV. CONSTRAINTS ON DARK ENERGY MODELS

Let us now present the 12 flat DE models whose free parameters will be constrained by using the same methodology and cosmological data as that applied to the ΛCDM model (see previous section).

A. Constant equation of state (XCDM model)

In this kind of cosmology (hereafter XCDM models) the equation of state parameter is constant [57]. In a point of fact, these DE models do not have a clear physical motivation. In particular, for quintessence models driven by a real scalar field, a constant EOS parameter requires an extreme fine-tuning of its potential and kinetic energy. In spite of that, this subclass of DE models has been widely used in the literature due to its simplicity. Notice that DE models with a canonical kinetic term have $-1 \leq w < -1/3$. Models with ($w < -1$), sometimes called phantom dark energy [58], are endowed with a very exotic nature, like a scalar field with negative kinetic energy. Now, by using Eq. (2.1) the normalized Hubble parameter becomes

---

[1]Likelihoods are normalized to their maximum values. In the present analysis we always report 1σ uncertainties on the fitted parameters. Note also that the total number of data points used here is $N_{\text{tot}} = 368$, while the associated degrees of freedom are: $\text{dof} = N_{\text{tot}} - n_{\text{fit}}$, with n_{fit} the model-dependent number of fitted parameters.

[2]Such a possibility has been crudely tested by Plionis *et al.* [54]. A lower value $\chi_{\text{SNIa}}^2/\text{dof} \simeq 1.07$ (similar to that of Davies [2]) has been obtained by increasing the distance modulus uncertainty of the *Constitution* nearby SNe Ia ($z \leq 0.4$) by 20%.

$$E^2(a) = \Omega_m a^{-3} + (1 - \Omega_m)a^{-3(1+w)}. \quad (4.1)$$

In order to constrain XCDM models with the observational data we sample $\Omega_m \in [0.1, 1]$ and $w \in [-2, -0.4]$ in steps of 0.01. As a result, we find that the best fit values are $\Omega_m = 0.28 \pm 0.01$ and $w = -0.99 \pm 0.05$ with $\chi^2_{\text{tot}}(\Omega_m, w)/\text{dof} \simeq 439.5/366$.

The above results are in excellent agreement with those found by different authors [2,4–6,8,31]. It is also worth noticing that the concordance ΛCDM cosmology is described by a XCDM model with w strictly equal to -1. The corresponding limits form the basis of our present comparison and were separately derived (see last section).

B. Parametric dark energy (CPL model)

This kind of cosmology was first discussed with basis on the Chevalier-Polarski-Linder [59,60] parametrization (hereafter CPL). The dark energy EOS parameter is defined as a first-order Taylor expansion around the present epoch,

$$w(a) = w_0 + w_1(1 - a), \quad (4.2)$$

where w_0 and w_1 are constants. The normalized Hubble parameter now reads

$$E^2(a) = \Omega_m a^{-3} + (1 - \Omega_m)a^{-3(1+w_0+w_1)}e^{3w_1(a-1)}. \quad (4.3)$$

In order to constrain the free parameters, we sample them as follows: $w_0 \in [-2, -0.4]$ and $w_1 \in [-2.6, 2.6]$ in steps of 0.01. By fixing a prior in the density parameter, $\Omega_m = 0.28$, we find that the overall likelihood function peaks at $w_0 = -0.96 \pm 0.13$ and $w_1 = -0.40 \pm 0.70$ in very good agreement with the 7 year WMAP data [5]. The corresponding $\chi^2_{\text{tot}}(w_0, w_1)/\text{dof}$ is 439.5/366. A value that should be compared with the ΛCDM prediction.

C. Braneworld gravity (BRG model)

In the context of a braneworld cosmology (hereafter BRG) the accelerated expansion of the Universe can be explained by a modification of the gravitational interaction in which gravity itself becomes weak at very large distances (close to the Hubble scale) due to the fact that our four-dimensional brane survives into an extra dimensional manifold (see [61] and references therein). The interesting aspect of this scenario is that the corresponding functional form of the normalized Hubble flow as given by Eq. (2.3) is affected only by one free parameter, Ω_m. The quantity δH^2 is given by

$$\delta H^2 = 2\Omega_{bw} + 2\sqrt{\Omega_{bw}}\sqrt{\Omega_m a^{-3} + \Omega_{bw}}, \quad (4.4)$$

where $\Omega_{bw} = (1 - \Omega_m)^2/4$. From Eq. (2.4), it is readily checked that the geometrical DE equation of state parameter reduces to

$$w(a) = -\frac{1}{1 + \Omega_m(a)}, \quad (4.5)$$

where $\Omega_m(a) \equiv \Omega_m a^{-3}/E^2(a)$. The joint likelihood analysis provides a best fit value of $\Omega_m = 0.23 \pm 0.01$, but the fit is much worse, $\chi^2_{\text{tot}}(\Omega_m)/\text{dof} \simeq 500/367$, in comparison with the one provided by a ΛCDM cosmology.

D. Low Ricci dark energy (LRDE model)

In this model we use a simple parametrization for the Ricci scalar which is based on a Taylor expansion around the present time: $\mathcal{R}(a) = r_0 + r_1(1 - a)$. It is interesting to mention that at the early epochs the cosmic evolution tends asymptotically to be matter dominated (for more details see [23]). In this framework, we have

$$E^2(a) = \begin{cases} a^{4(r_0+r_1-1)}e^{4r_1(1-a)} & a \geq a_t \\ \Omega_m a^{-3} & a < a_t, \end{cases} \quad (4.6)$$

where $a_t = 1 - (1 - 4r_0)/4r_1$. At present, the matter density parameter is directly related with the above constants via

$$\Omega_m = \left(\frac{4r_0 + 4r_1 - 1}{4r_1}\right)^{4r_0+4r_1-1}e^{1-4r_0}. \quad (4.7)$$

The corresponding EOS parameter is given by

$$w(a) = \frac{1 - 4\mathcal{R}(a)}{3}\left[1 - \Omega_m e^{-\int_a^1 d\ln y(1-4\mathcal{R})}\right]^{-1}. \quad (4.8)$$

Notice, that we sample the unknown parameters as follows: $r_0 \in [0.5, 1.5]$ and $r_1 \in [-2.4, -0.1]$ and here are the results: $r_0 = 0.80 \pm 0.02$ and $r_1 = -0.69 \pm 0.05$ ($\Omega_m \simeq 0.27$) with $\chi^2_{\text{tot}}(r_0, r_1)/\text{dof} \simeq 439.9/366$.

E. High Ricci dark energy (HRDE model)

A different Ricci DE model was proposed by Linder and Cahn [62]. In this framework, the Ricci scalar evolves at high redshifts obeying the following expression:

$$\mathcal{R} \simeq \frac{1}{4}\left[1 - 3w_0\frac{\delta H^2}{H^2}\right], \quad (4.9)$$

where $\delta H^2 = E^2(a) - \Omega_m a^{-3}$. In this model the normalized Hubble flow becomes

$$E^2(a) = \Omega_m a^{-3}(1 + \beta a^{-3w_0})^{-\ln \Omega_m/\ln(1+\beta)}, \quad (4.10)$$

where $\beta = \Omega_m^{-1} - 1$. As in the previous case, the effective equation of state parameter is again related to $E(a)$ according to Eq. (2.2). Now, by using the same sampling as in the XCDM models, we find that the joint likelihood peaks at $\Omega_m = 0.28 \pm 0.01$ and $w_0 = -0.99 \pm 0.05$ with $\chi^2_{\text{tot}}(\Omega_m, w_0)/\text{dof} \simeq 439.5/366$.

F. Tension of cosmic magnetic fields (TCM model)

A few years ago, Contoupolos and Basilakos [63] proposed a novel idea which is based on the following consideration (hereafter TCM): if the cosmic magnetic field is generated in sources (such as galaxy clusters) whose overall dimensions remain unchanged during the expansion of the Universe, the stretching of this field by the cosmic expansion generates a tension (negative pressure) that could possibly explain a small fraction of the DE (~ 2–5%). In this flat cosmological scenario the normalized Hubble flow becomes

$$E^2(a) = \Omega_m a^{-3} + \delta H^2, \qquad \delta H^2 = \Omega_\Lambda + \Omega_B a^{-3+n},$$
$$(4.11)$$

where Ω_B is the density parameter for the cosmic magnetic fields and $\Omega_\Lambda = 1 - \Omega_m - \Omega_B$. From Eq. (2.4) it is readily seen that the effective EOS parameter which is related to magnetic tension reads

$$w(a) = -\frac{3\Omega_\Lambda + n\Omega_B a^{-3+n}}{3(\Omega_\Lambda + \Omega_B a^{-3+n})}. \qquad (4.12)$$

Again, in order to constrain the parameters, we sample $\Omega_B \in [0., 0.3]$ and $n \in [0, 10]$. By considering a prior of $\Omega_m = 0.28$, the best fit values are: $\Omega_B = 0.01 \pm 0.005$ and $n = 1.80 \pm 0.80$ with $\chi^2_{\text{tot}}(\Omega_B, n)/\text{dof} \simeq 439.8/366$.

G. Pseudo-Nambu Goldstone Boson (PNGB model)

In this cosmological model the DE equation of state parameter is expressed with the aid of the potential $V(\phi) \propto [1 + \cos(\phi/F)]$ [64],

$$w(a) = -1 + (1 + w_0)a^F, \qquad (4.13)$$

where $w_0 \in [-2, -0.4]$ and $F \in [0, 8]$. We see that for $a \ll 1$, the EOS parameter goes to $w(a) = -1$. Based on this parametrization the quantity δH^2 [see Eq. (2.4)] takes the following form:

$$\delta H^2 = (1 - \Omega_m) \exp\left[\frac{3(1 + w_0)}{F}(1 - a^F)\right]. \qquad (4.14)$$

In this case, our joint statistical analysis yields that the likelihood function peaks at $w_0 = -0.97 \pm 0.09$ and $F = 5.9 \pm 3.2$ with $\chi^2_{\text{tot}}(w_0, F)/\text{dof} \simeq 439.7/366$.

H. Early dark energy (EDE model)

Another cosmological scenario that we include in our paper is the early dark energy model (hereafter EDE). The basic assumption here is that at early epochs the amount of DE is not negligible [65]. In this framework, the overall DE component is given by

$$\Omega_{\text{DE}}(a) = \frac{1 - \Omega_m - \Omega_e(1 - a^{-3w_0})}{1 - \Omega_m + \Omega_m a^{3w_0}} + \Omega_e(1 - a^{-3w_0}),$$
$$(4.15)$$

where Ω_e is the early DE density and w_0 is the equation of state parameter at the present epoch. We observe that the EDE model was designed to satisfy the two following conditions: (i) mimic the effects of a late dark energy, and (ii) provide a decelerating expansion of the Universe at high redshifts. The normalized Hubble parameter is now written as

$$E^2(a) = \frac{\Omega_m a^{-3}}{1 - \Omega_{\text{DE}}(a)}, \qquad (4.16)$$

and from Eq. (2.2), one may obtain the EOS parameter as a function of the scale factor.

Now, from the joint likelihood analysis we find that $\Omega_e = 0.02 \pm 0.02$ and $w_0 = -1.04^{+0.07}_{-0.11}$ (for the prior of $\Omega_m = 0.28$) with $\chi^2_{\text{tot}}(\Omega_e, w_0)/\text{dof} \simeq 439.3/366$. Note, that a different class of EDE models was recently studied in [45].

I. Variable Chaplygin gas (VCG model)

Accelerating cosmologies can also be driven by the so-called variable Chaplygin gas (hereafter VCG) which corresponds to a Born-Infeld tachyon action [21,66]. Recently, an interesting family of Chaplygin gas models was found to be consistent with the current observational data [67]. In the framework of a spatially flat geometry, it can be shown that the normalized Hubble function takes the following formula:

$$E^2(a) = \Omega_b a^{-3} + (1 - \Omega_b)\sqrt{B_s a^{-6} + (1 - B_s)a^{-n}},$$
$$(4.17)$$

where $\Omega_b \simeq 0.0226h^{-2}$ is the density parameter for the baryonic matter [5] and $B_s \in [0.01, 0.51]$ and $n \in [-4, 4]$. The effective matter density parameter is $\Omega_m = \Omega_b + (1 - \Omega_b)\sqrt{B_s}$. We find that the best fit parameters are $B_s = 0.05 \pm 0.01$ and $n = 1.65^{+0.19}_{-0.25}$ ($\Omega_m \simeq 0.26$) with $\chi^2_{\text{tot}}(B_s, n)/\text{dof} \simeq 441.3/366$.

J. Time-varying vacuum (Λ_{RG} and Λ_{PS}) models

Let us now consider the possibility of a decaying Λ cosmology, that is, $\Lambda = \Lambda(a)$. In this kind of model, the value of Λ is small because the Universe is too old and, therefore, it alleviates the cosmological constant problem. As it appears, the decaying vacuum equation of state does not depend on whether Λ is strictly constant or variable. Therefore, the EOS takes the usual form, $P_\Lambda(t) = -\rho_\Lambda(t) = -\Lambda(t)/8\pi G$. The global dynamics of such models has been investigated extensively in the literature, in fact, much before the discovery of the present accelerating stage [13] (for a recent and extensive discussion see Basilakos *et al.* [14]). By introducing in the Friedmann equations the idea of a time-dependent vacuum one obtains

$$\dot{H} + \frac{3}{2}H^2 = \frac{\Lambda}{2}. \tag{4.18}$$

The traditional $\Lambda = \mathrm{const}$ cosmology can be described directly by the integration of Eq. (4.18), but the same equation is also valid for $\Lambda = \Lambda(a)$. This means that a supplementary equation for the time evolution of Λ is needed in order to unveil the dynamics of this pattern. In this work we consider two different versions of the $\Lambda(a)$ models, namely, the renormalization group of the quantum field vacuum [25,68] (hereafter Λ_{RG}) and a power series vacuum [69] (hereafter Λ_{PS})

$$\Lambda(H) = \begin{cases} \Lambda_0 + 3\gamma(H^2 - H_0^2) & \text{for } \Lambda_{\mathrm{RG}} \\ H_0(\gamma - 3\Omega_m)H + (3 - \gamma)H^2 & \text{for } \Lambda_{\mathrm{PS}}. \end{cases} \tag{4.19}$$

Naturally, the vacuum energy density is normalized to its present value, $\Lambda_0 \equiv \Lambda(H_0) = 3\Omega_\Lambda H_0^2$ ($\Omega_\Lambda = 1 - \Omega_m$). Inserting the above expressions into Eq. (4.18) we finally obtain the normalized Hubble flow

$$E(a) = \begin{cases} \left[\frac{1-\Omega_m-\gamma}{1-\gamma} + \frac{\Omega_m}{1-\gamma}a^{-3(1-\gamma)}\right]^{1/2} & \text{for } \Lambda_{\mathrm{RG}} \\ 1 - \frac{3\Omega_m}{\gamma} + \frac{3\Omega_m}{\gamma}a^{-\gamma/2} & \text{for } \Lambda_{\mathrm{PS}}. \end{cases} \tag{4.20}$$

It has been shown [68,70] that for $\Lambda(t)$ there is a coupling between the time-dependent vacuum and matter component. Indeed, by combining the conservation of the total energy with the variation of the vacuum energy, one can shown that the $\Lambda(t)$ models provide either a particle production process or that the mass of the dark matter particles increases [71].

Now, by applying our statistical procedure for both cosmologies, the best fit parameters are:

Λ_{RG} model: $\Omega_m = 0.28 \pm 0.01$ and $\gamma = 0.002 \pm 0.001$ with $\chi^2_{\mathrm{tot}}(\Omega_m, \gamma)/\mathrm{dof} \simeq 439.5/366$.

Λ_{PS} model: $\Omega_m = 0.32 \pm 0.02$ and $\gamma = 3.45^{+0.02}_{-0.03}$ with $\chi^2_{\mathrm{tot}}(\Omega_m, \gamma)/\mathrm{dof} \simeq 440.7/366$.

K. Creation cold dark matter (CCDM model)

In the context of the standard general relativity theory, is also possible to reduce the dark sector by considering the presence of the gravitationally induced particle creation mechanism. Like $\Lambda(t)$ models, this kind of scenario was also discussed long ago [72]. More recently, the cosmological equations for the mixture of radiation, baryons and cold dark matter (with creation of dark matter particles), and the energy conservation laws for each component have been investigated thoroughly in [73–75]. In this framework, the basic equation governing the global dynamics of a Universe endowed with a flat geometry is [73–76]

$$\dot{H} + \frac{3}{2}H^2 = \frac{4\pi G\rho_{dm}}{3}\frac{\Gamma}{H}, \tag{4.21}$$

where ρ_{dm} is the dark matter energy densities and Γ is the so-called creation rate of the cold dark matter and it has

units of $(\mathrm{time})^{-1}$. The creation pressure is negative and defined in terms of the creation rate and other cosmological quantities by the expression [73–76]

$$p_c = -\frac{\rho_{\mathrm{dm}}\Gamma}{3H}. \tag{4.22}$$

In CCDM models, the functional form of Γ is phenomenologically parametrized [75] by the following relation:

$$\Gamma = 3\tilde{\Omega}_\Lambda\left(\frac{\rho_{\mathrm{co}}}{\rho_{\mathrm{dm}}}\right)H, \tag{4.23}$$

where $\tilde{\Omega}_\Lambda$ (called α in Ref. [75]) is a constant, $\rho_{\mathrm{co}} = 3H_0^2/8\pi G$ is the present-day value of the critical density. Performing now the integration of Eq. (4.21) we obtain

$$E^2(a) = \tilde{\Omega}_m a^{-3} + \tilde{\Omega}_\Lambda, \tag{4.24}$$

where $\tilde{\Omega}_\Lambda = 1 - \tilde{\Omega}_m$. Interestingly, the CCDM model resembles the global dynamics of the concordance ΛCDM cosmology by including only one free parameter. In particular, this means that $\tilde{\Omega}_m = 0.28 \pm 0.01$ with $\chi^2_{\mathrm{tot}}(\tilde{\Omega}_m)/\mathrm{dof} \simeq 439.6/367$.

V. EVOLUTION OF MATTER PERTURBATIONS

In this section we generalize the basic equations which govern the behavior of the matter perturbations within the framework of the previously described DE models. We focus our attention on the most generic models, i.e., the $\Lambda(t)$ and CCDM models. In these cases, a neo-Newtonian description can be introduced by considering an extended continuity equation together with the Euler and Poisson equations [77,78]. By introducing the particle creation model, the evolution equation of the growth factor becomes [14,76]

$$\ddot{D} + (2H + Q)\dot{D} - (4\pi\tilde{G}\rho_m - 2HQ - \dot{Q})D = 0, \tag{5.1}$$

where ρ_m is the matter density, $\tilde{G} = G$, and

$$Q(t) = \begin{cases} -\dot{\Lambda}/\rho_m & \text{for } \Lambda_{\mathrm{RG}} \text{ or } \Lambda_{\mathrm{PS}} \\ 3\tilde{\Omega}_\Lambda\rho_{co}H/\rho_m & \text{for CCDM}. \end{cases} \tag{5.2}$$

In the case of noninteracting DE models, $[Q(t) = 0, \tilde{G} = G]$, the above equation (5.1) reduces to the usual time evolution equation for the mass density contrast [48,79,80], while in the case of the geometrical DE models $[Q(t) = 0, \tilde{G} = G_{\mathrm{eff}}]$ (e.g., [81]).

Useful expressions of the growth factor have been given by Peebles [80] for the ΛCDM cosmology. Several works have also derived the growth factor for $w = \mathrm{const}$ DE models [82–85], and for the braneworld cosmology [86]. Linder [23] and Linder and Cahn [62] derived similar expressions for dark energy models in which the Ricci scalar varies with time (and which we use in the current study), as well as for models with a time-varying equation of state, while for the scalar tensor models the growth

factor was obtained by Gannouji and Polarski [87]. For the interacting DE models we use the growth factors which were recently derived in [14,41,76].[3]

VI. HALO ABUNDANCES AND THEIR EVOLUTION IN DARK ENERGY MODELS

In this section we derive the cluster-size halo number counts and their corresponding redshift distribution within the framework of the DE models analyzed in this work. We will then compare our predictions with those of the conventional ΛCDM cosmology. In principle, this can help us to understand better the theoretical expectations of the current DE models, as well as to identify the realistic variants of the concordance ΛCDM cosmology.

An important theoretical question in cosmology is how to determine the fraction of matter in the Universe that has formed bounded structures, and what is its distribution in mass at any given redshift after recombination? The simplest successful answer to this question was given in 1974 by Press and Schechter [88] (hereafter PSc). In their approach, the primordial density fluctuations for a given mass M on the dark matter fluid is described by a random Gaussian field. The function $F(M, z)$ represents the fraction of the Universe that has collapsed by the redshift z in halos above some mass M. With this function one may estimate the number density of halos $n(M, z)$ with masses within the range $(M, M + \delta M)$,

$$n(M, z)dM = \frac{\partial \mathcal{F}(M, z)}{\partial M} \frac{\bar{\rho}}{M} dM. \tag{6.1}$$

Performing the differentiation and after some algebra one obtains the following:

$$\begin{aligned} n(M, z)dM &= -\frac{\bar{\rho}}{M}\left(\frac{1}{\sigma}\frac{d\sigma}{dM}\right)f_{\text{PSc}}(\sigma)dM \\ &= \frac{\bar{\rho}}{M}\frac{d\ln\sigma^{-1}}{dM}f_{\text{PSc}}(\sigma)dM, \end{aligned} \tag{6.2}$$

where $f_{\text{PSc}}(\sigma) = \sqrt{2/\pi}(\delta_c/\sigma)\exp(-\delta_c^2/2\sigma^2)$, δ_c is the linearly extrapolated density threshold above which structures collapse [89], while $\sigma^2(M, z)$ is the mass variance of the smoothed linear density field, extrapolated to redshift z at which the halos are identified. It is given in Fourier space by

$$\sigma^2(M, z) = \frac{D^2(z)}{2\pi^2}\int_0^\infty k^2 P(k)W^2(kR)dk, \tag{6.3}$$

where $D(z)$ is the growth factor of perturbations, $P(k)$ is the power spectrum of the linear density field, $W(kR) = 3(\sin kR - kR\cos kR)/(kR)^3$ is the top-hat smoothing function which contains on average a mass M within a radius $R = (3M/4\pi\bar{\rho})^{1/3}$, and $\bar{\rho} = 2.78\times 10^{11}\Omega_m h^2 M_\odot$ Mpc^{-3}. We use the CDM power spectrum, $P(k) = P_0 k^n T^2(\Omega_m, k)$, with $T(\Omega_m, k)$ the CDM transfer function (according to [90]), $n \simeq 0.96$, following the 7-year WMAP results [5], and

$$P_0 \simeq 2.2 \times 10^{-9}\left(\frac{2}{5\Omega_m}\right)^2 H_0^{-4} k_{\text{WMAP}}^{1-n}, $$

where $k_{\text{WMAP}} = 0.02$ Mpc^{-1} is a characteristic wavelength, given in [5]. Note that in this approach all the mass is locked inside halos, according to the normalization constraint

$$\int_{-\infty}^{+\infty} f_{\text{PSc}}(\sigma)d\ln\sigma^{-1} = 1. \tag{6.4}$$

Although the above (Press-Schechter) formulation was shown to give a reasonable approximation to the expectations provided by numerical simulations, it was later found to overpredict/underpredict the number of low/high mass halos at the present epoch [91,92].

More recently, a many works have provided better fitting functions of $f(\sigma)$, some of them based on a phenomenological approach. In the present treatment, we adopt the one proposed by Reed et al. [93].

A. Collapse threshold and mass variance of DE models

In order to compare the mass function predictions of the different DE models, it is imperative to use for each model the corresponding values of δ_c and $\sigma^2(M, z)$. In the Press-Schechter formalism, the rms matter fluctuations are parametrized at redshift $z = 0$ so that one has for any cosmological model

$$\sigma^2(M, z) = \sigma_8^2(z)\frac{\Psi(\Omega_m, R)}{\Psi(\Omega_m, R_8)}, \tag{6.5}$$

with

$$\Psi(\Omega_m, R) = \int_0^\infty k^{n+2}T^2(\Omega_m, k)W^2(kR)dk \tag{6.6}$$

and

$$\sigma_8(z) = \sigma_8(0)\frac{D(z)}{D(0)}, \tag{6.7}$$

where $\sigma_8(0)[\equiv \sigma_8]$ the rms mass fluctuation on $R_8 = 8h^{-1}$ Mpc scales at redshift $z = 0$. Therefore, for a given perturbed DE model, it is not enough to consider its growing mode, $D(z)$, but one has also to obtain the corresponding σ_8 value. Below the parameters $D_{\text{DE}}(z)$, $\sigma_{8,\text{DE}}$ denote

---

[3]For many DE models, it is convenient to study the growth evolution in terms of the expansion scale a or characteristic scale $\ln a$, rather than t. As an example, in the case of the braneworld cosmology, Linder and Cahn [62] used $g = d\ln(D/a)/d\ln a$ (see their eqs. 8, 20, and 27), while for the LRDE and HRDE models, Linder [23] utilized $g = D/a$ (see eq. 31 in their paper). Since the pure matter universe (Einstein de Sitter) has the solution of $D_{\text{EdS}} = a$, we normalize our DE models so as to get $D \simeq a$ at large redshifts due to the dominance of the nonrelativistic matter component (e.g., $z = 30$, where the DE density is almost negligible and the radiation density is less than $\sim 1\%$ of the matter density).

the growth factor and the rms mass perturbation normalization of the DE models, while $D_\Lambda(z)$, $\sigma_{8,\Lambda}$ denote the corresponding quantities for the reference ΛCDM model.

1. The relevant DE model δ_c values

It is well known that in the conventional Λ cosmology $\delta_c \simeq 1.675$, while Weinberg and Kamionkowski [38] provide an accurate fitting formula to estimate δ_c for any DE model with a constant equation of state parameter (see their Eq. 18). Let us now discuss the values of the linearly extrapolated density δ_c adopted here for the different DE models.

First, since for the Λ_{RG}, Λ_{PS}, and CCDM models, the EOS parameter is strictly equal to -1, we are completely justified to use $\delta_c \simeq 1.675$. Using literature data we also find: (i) for the BRG model $\delta_c \simeq 1.667$ [94]; (ii) for the EDE model, $\delta_c \simeq 1.672$ [44]; (iii) for the CPL model, $\delta_c \simeq 1.663$ [44]; and (iv) for the VCG model, $\delta_c \simeq 1.642$ [44]. Interestingly, one can check that the above δ_c values can be well approximated using the previously discussed fitting formula [38], despite the fact that it was derived for a constant equation of state parameter. As an example, in the case of the BRG geometrical model the fitting formula predicts $\delta_c \simeq 1.667$, which is in excellent agreement with that found by the theoretical analysis of Schmidt et al. [94].

Second, for the rest of the dark energy models (LRDE, TCM, PNGB, and HRDE) there are, to our knowledge, no available δ_c values in the literature, which implies that one has to study in detail the spherical collapse model in order to estimate their exact δ_c values, something which is beyond the scope of the present paper. However, since in these models $w \simeq -1$ close to the present epoch, we have decided to adopt the Weinberg and Kamionkowski formula because it appears to work quite well. In this case, for the

remaining DE models (LRDE, TCM, PNGB, and HRDE) we have derived $\delta_c \simeq 1.674$.

2. Estimation of the different DE model σ_8

The different DE models σ_8 value can be estimated by scaling the present time $(z = 0)$ $\sigma_{8,\Lambda}$ value to that relevant to each DE model by using Eq. (6.3) at the present time. We again have that

$$\sigma_{8,DE} = \sigma_{8,\Lambda} \frac{D_{DE}(0)}{D_\Lambda(0)} \sqrt{\frac{P_{DE,0}}{P_{\Lambda,0}} \frac{\Psi(\Omega_m, R_8)}{\Psi(\Omega_{m,\Lambda}, R_8)}}, \qquad (6.8)$$

with $\Omega_{m,\Lambda}$ denoting the value for the reference Λ model (in our case $\Omega_{m,\Lambda} = 0.28$; see Sec. III), while we have (for fixed H_0, as in our case) that

$$\left(\frac{P_{DE,0}}{P_{\Lambda,0}}\right)^{1/2} = \frac{\Omega_{m,\Lambda}}{\Omega_m}. \qquad (6.9)$$

It thus follows that if the $\sigma_{8,\Lambda}$ value is known, one may derive the corresponding $\sigma_{8,DE}$ values to the other DE models. In this concern, the combined SNIa + BAO + WMAP5 analysis of Komatsu et al. [5] (see also [95]) provided a value of $\sigma_{8,\Lambda} \simeq 0.812$, while the corresponding WMAP7 analysis yielded [for $w(z) = -1$]: $\sigma_{8,\Lambda} \simeq 0.803$ (using the WMAP7 alone) and $\sigma_8 \simeq 0.807$ for the joint WMAP7 + BAO + H_0 analysis [5]. A recent analysis based on cluster abundances has also furnished the following degenerate combination: $\sigma_{8,\Lambda} = 0.83 \pm 0.03(\Omega_{m,\Lambda}/0.25)^{-0.41}$ [96], which for our case ($\Omega_{m,\Lambda} = 0.28$) implies $\sigma_{8,\Lambda} \simeq 0.792$. Fu et al. [97] based on a weak-lensing procedure found $\sigma_{8,\Lambda} = 0.837 \pm 0.084(\Omega_{m,\Lambda}/0.25)^{-0.53}$ which implies $\sigma_{8,\Lambda} \simeq 0.788$ in our case. In addition, studies based on the peculiar velocities statistical analysis [98] obtained $\sigma_{8,\Lambda} = 0.88 \pm$

TABLE I. Numerical results. The first column indicates the DE model. The second column gives symbols or line types of the models appearing in Figs. 1–3. The third and fourth columns show the $\sigma_{8,DE}$ and δ_c values. The remaining columns present the fractional relative difference between the models and the ΛCDM cosmology for two future cluster surveys discussed in the text. Bold letters denote those models that can be clearly distinguished from a flat ΛCDM model at some redshift bin (uncertainties appear only when their value is $\geq 10^{-2}$).

Model	Symbol	$\sigma_{8,DE}$	δ_c	$(\delta\mathcal{N}/\mathcal{N}_\Lambda)_{eROSITA}$			$(\delta\mathcal{N}/\mathcal{N}_\Lambda)_{SPT}$		
				$z < 0.5$	$0.5 \leq z < 1$	$1 \leq z < 1.5$	$z < 0.5$	$0.5 \leq z < 1$	$1 \leq z < 1.5$
XCDM	black thin line	0.802	1.675	−0.01	0.00	0.01 ± 0.02	−0.01	0.00	0.00
BRG	blue short-dashed line	0.523	1.667	−0.95	−1.00	−1.00	−0.95	−0.98	−0.99
CPL	green dashed line	0.821	1.663	0.11	0.19	0.28 ± 0.02	0.11	0.16	0.19
LRDE	red x	0.784	1.674	−0.14	−0.19	-0.28 ± 0.01	−0.14	−0.17	−0.21
HRDE	cyan stars	0.798	1.674	−0.01	−0.01	0.00 ± 0.02	−0.02	−0.01	0.00
TCM	magenta dashed line	0.799	1.674	−0.02	−0.02	-0.02 ± 0.02	−0.02	−0.02	−0.02
PNGB	red small dots	0.802	1.674	0.00	0.01	0.03 ± 0.02	0.00	0.01	0.01
EDE	blue long-dashed line	0.755	1.672	−0.22	−0.41	-0.66 ± 0.01	−0.22	−0.34	−0.49
VCG	black squares	0.764	1.642	−0.23	−0.33	-0.56 ± 0.01	−0.23	−0.29	−0.43
Λ_{PS}	red circles	1.017	1.675	2.00	14.3 ± 0.02	440 ± 5	1.89	7.5	35.3
Λ_{RG}	black thick line	0.795	1.675	−0.05	−0.11	-0.22 ± 0.01	−0.05	−0.08	−0.14
CCDM	magenta stars	0.564	1.675	−0.59	−0.69	−0.94	−0.56	−0.62	−0.87

$0.05(\Omega_{m,\Lambda}/0.25)^{-0.53}$ or $\sigma_{8,\Lambda} \simeq 0.829$ in our case. It should be stressed that the average scattering of the four independent $\sigma_{8,\Lambda}$ values (of those based on WMAP, we use only the joint WMAP7 + BAO + H_0 result) is quite small ($\langle\sigma_{8,\Lambda}\rangle \simeq 0.804 \pm 0.018$), thereby reinforcing the consistency of the different measurements. Finally, by inserting the latter value in Eq. (6.8) we can estimate the corresponding $\sigma_{8,DE}$ values, listed in Table I, to be used in our mass function analysis.

For completeness, it should be remarked that some recent analyses are suggesting significantly higher values of σ_8. For example, Watkins *et al.* [99] studying the bulk flow on scales of $\sim 100h^{-1}$ Mpc found a σ_8 normalization which is increased by a factor of ~ 2 with respect to the one of the ΛCDM model. If these results are correct, the ΛCDM model would be strongly challenged. However, such a discussion is beyond the scope of the current work.

B. Halo mass function and number counts of DE models

We now pass to our results. In the upper panels of Fig. 1, for two different redshifts ($z = 0.5$ and 2), we display the integral halo mass function, $n(>M)$, for all DE models previously discussed. The different models are characterized by the symbols and line types presented in Table I.

In the corresponding lower panels one may see the fractional difference between each DE model with the concordance ΛCDM model, that is, $\delta n/n_\Lambda = (n_{DE} - n_\Lambda)/n_\Lambda$. We stress that we have shown the case $z = 2$ only for comparison of the model expectations. In other words, it is not a statement of the viability to actually observe clusters at such a large redshift (not only due to
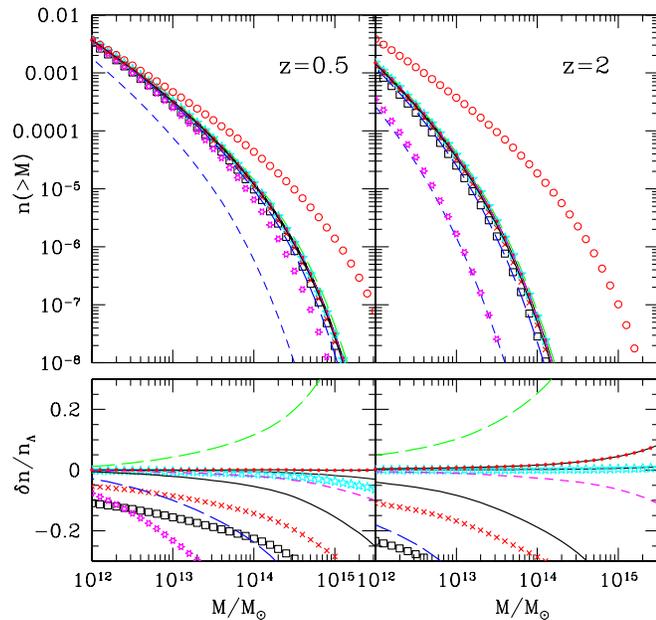

FIG. 1 (color online).   The halo mass function at two different redshifts. The different DE models are represented by different symbols and/or line types (see Table I for definitions).

technical limitations but also because the majority of dark matter halos is not expected to have virialized at such a redshift, thereby producing their X-ray signatures).

It is worth noticing the mass function expectation of the Λ_{PS} model (open red circles), the BRG model (blue dashed line), and at high redshifts of the CCDM model (magenta stars) appears to be completely different from the reference ΛCDM cosmology.

Given the halo mass function we can now derive an observable quantity which is the redshift distribution of clusters, $\mathcal{N}(z)$, within some determined mass range, say $M_1 \leq M/M_\odot \leq M_2$. This can be estimated by integrating, in mass, the expected differential halo mass function, $n(M, z)$, according to

$$\mathcal{N}(z) = \frac{dV}{dz} \int_{M_1}^{M_2} n(M, z)dM, \qquad (6.10)$$

where dV/dz is the comoving volume element, which in a flat universe takes the form

$$\frac{dV}{dz} = 4\pi r^2(z)\frac{dr}{dz}(z), \qquad (6.11)$$

with $r(z)$ denoting the comoving radial distance out to redshift z,

$$r(z) = \frac{c}{H_0} \int_0^z \frac{dx}{E(x)}. \qquad (6.12)$$

In Fig. 2 (upper panel), we show the theoretically expected cluster redshift distribution, $\mathcal{N}(z)$, for all the models studied (line and symbol types are listed in Table I), for cluster of galaxies size halos, i.e., $M_1 = 10^{14}M_\odot$ and $M_2 = 10^{16}M_\odot$. It is evident that many of the different models show significant differences with respect to the concordance Λ model and therefore we could, in principle, distinguish them. In the lower panel of Fig. 2 we show the relative differences of the various DE models with respect to the expectations of the concordance ΛCDM model. Note that the three models (Λ_{PS}, CCDM, and BRG models), for which we found very large mass function differences (Fig. 1), are not shown because their large relative differences are beyond the limits of the lower panel.

Let us now discuss the expected redshift distributions, based on two future cluster surveys, and also the possibility to observationally discriminate the different DE models.

These two realistic future surveys are: (a) the eROSITA satellite X-ray survey, with a flux limit of $f_{lim} = 3.3 \times 10^{-14}$ ergs s^{-1} cm^{-2}, at the energy band 0.5–5 keV and covering $\sim 20\,000$ deg^2 of the sky; and (b) the South Pole Telescope SZ survey, with a limiting flux density at $\nu_0 = 150$ GHz of $f_{\nu_0,lim} = 5$ mJy and a sky coverage of ~ 4000 deg^2.

To realize the predictions of the first survey we use the relation between halo mass and bolometric X-ray luminosity, as a function of redshift, provided in [100], i.e.,
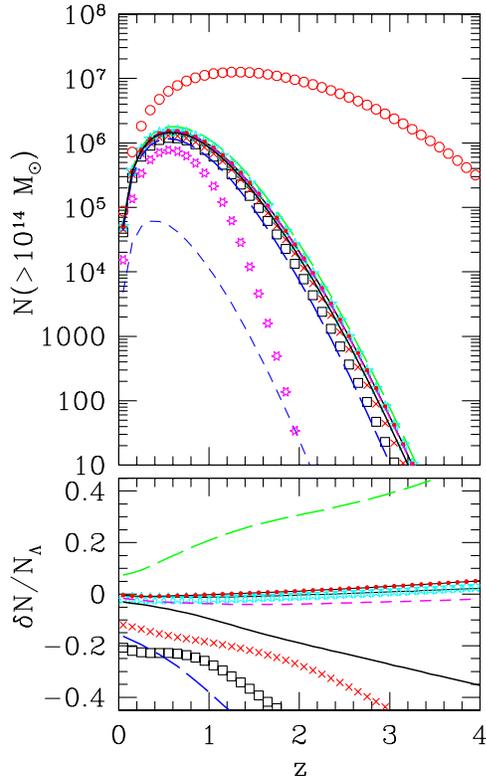
FIG. 2 (color online).   The expected redshift distribution of $M \gtrsim 10^{14} M_\odot$ clusters (upper panel) of the different DE models and the corresponding fractional difference between the models and the reference ΛCDM model (lower panel). The lower panel shows only those DE models that have fractional relative differences, with respect to the ΛCDM model, of $\lesssim 45\%$. Symbols correspond to the different DE models as indicated in Table I.

$$L(M, z) = 3.087 \times 10^{44} \left[\frac{ME(z)}{10^{15} h^{-1} M_\odot} \right]^{1.554} h^{-2} \text{ erg s}^{-1}.$$

$$(6.13)$$

The limiting halo mass that can be observed at redshift z is then found by inserting in the above equation the limiting luminosity, given by $L = 4\pi d_L^2 f_{\text{lim}} c_b$, with d_L the luminosity distance corresponding to the redshift z and c_b the band correction, necessary to convert the bolometric luminosity of Eq. (6.13) to the 0.5–5 keV band of eROSITA. We estimate this correction by assuming a Raymond-Smith (1977) plasma model with a metallicity of $0.4 Z_\odot$, a typical cluster temperature of ~ 4 keV, and a Galactic absorption column density of $n_H = 10^{21}$ cm^{-2}.

The predictions of the second survey can be realized using again the relation between limiting flux and halo mass from [100],

$$f_{\nu_0, \text{lim}} = \frac{2.592 \times 10^8 \text{ mJy}}{d_A^2(z)} \left(\frac{M}{10^{15} M_\odot} \right)^{1.876} E^{2/3}(z), \quad (6.14)$$

where $d_A(z) \equiv d_L/(1 + z)^2$ is the angular diameter distance out to redshift z.

In Fig. 3 (upper panel) we present the expected redshift distributions above a limiting halo mass, which is $M_1 \equiv M_{\text{limit}} = \max[10^{14} M_\odot, M_f]$, with M_f corresponding to the mass related to the flux limit at the different redshifts, estimated by solving Eqs. (6.13) and (6.14) for M. In the lower panels we present the fractional difference between the different DE models and ΛCDM, similarly to Fig. 2, but now for the realistic case of the previously mentioned future cluster surveys. It is evident that the imposed flux limits together with the scarcity of high mass halos at large redshifts, induce an abrupt decline of $\mathcal{N}(z)$ with z, especially in the case of the eROSITA X-ray survey (note the shallower redshifts depicted in Fig. 3 with respect to Fig. 2).

In the lower panels of Fig. 3 we display the relative differences of the DE models but only up to a redshift at which they are significant, that is, such that

$$\frac{\mathcal{N}_{\text{DE}} - \mathcal{N}_\Lambda}{(\mathcal{N}_{\text{DE}} - \mathcal{N}_\Lambda)^{1/2}} > 3.5, \quad (6.15)$$

with $\mathcal{N}_{\text{DE}}$ the redshift distribution predicted by some DE model and $\mathcal{N}_\Lambda$ the corresponding redshift distribution of ΛCDM model. However, such a criterion does not take into account cosmic variance and possible observational systematic uncertainties which can hamper detecting small [but according to Eq. (6.15) significant] relative differences. We believe that relative differences of $\lesssim 5\%$ will be difficult to detect especially at relative high redshifts.

In Table I, one may see a more compact presentation of our results including the relative fractional difference
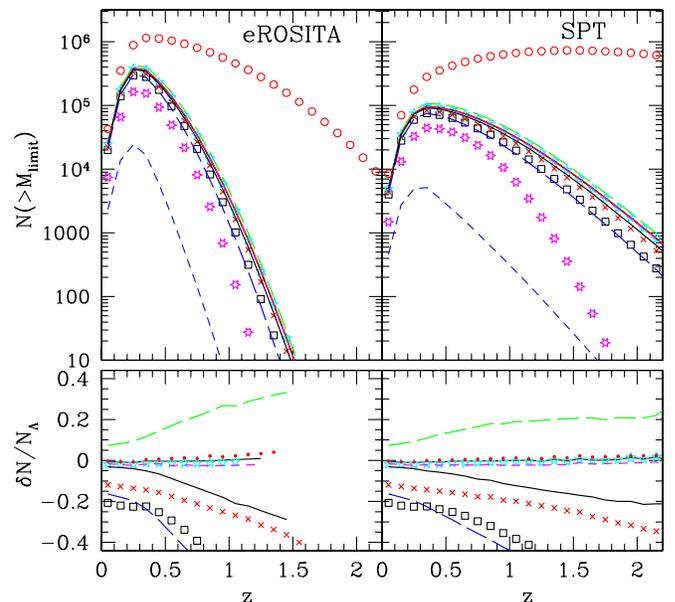

FIG. 3 (color online).   The expected cluster redshift distribution of the different DE models and for the two different future cluster surveys (upper panels), and the corresponding fractional difference with respect to the reference ΛCDM model (lower panels). Symbols correspond to the different DE models as indicated in Table I.

between all DE models and the ΛCDM model, in 3 distinct redshift bins and for both future surveys.

Based on our $\mathcal{N}(z)$ analysis and the results presented in Fig. 3 and Table I, we can now divide the studied DE models into those that can be distinguished observationally and those that are practically indistinguishable from the current paradigm (ΛCDM). The latter DE models are the following four: XCDM, HRDE, TCM, and PNGB. One has to remember however that these results are based on using DE model parameters that have been fitted by the present-day cosmological data (see Sec. IV). As an illustrative example, we remind the reader that the XCDM model, compared here, is one with $w = -0.99$; if future cosmological data would provide a different value for the equation of state parameter then the $N(z)$ predictions of such an XCDM model could be quite different than those derived here.

Regarding the models that are distinguishable with respect to the concordance model, three of them (BRG, Λ_{PS}, and CCDM) show extremely large variations making it trivial to distinguish them. From the rest of the distinguishable DE models all of them show clear signs of difference, at all redshifts and in both future cluster surveys, with respect to the ΛCDM expectations; only the Λ_{RG} model needs to be distinguished at higher redshifts ($z \gtrsim 0.5$).

As an additional test and in order to check the sensitivity of our results only on the functional form of the DE equation of state parameter, we have imposed a unique value of the rms mass fluctuation normalization to all DE models according to: $\sigma_{8,DE} = \sigma_{8,\Lambda}$, and repeated the cluster-size halo $N(z)$ analysis. We now find slightly different results although in the same overall direction with our main analysis. For example, the DE models that cannot be distinguished from the reference ΛCDM model are now the XCDM, TCM, PNGB, EDE, and Λ_{RG}, with the first three being common in both analyses, the Λ_{RG} model showing a small difference and the EDE being the only model that shows a significantly different behavior between the two analyses.

Finally we would like to mention that an interesting paper appeared recently [101] and among other issues, it compares different forms of the halo mass function and its redshift evolution using N-body simulations of the ΛCDM and wCDM ($w = $ const) models. The authors do find some differences at the few percent level. Although our analysis is self-consistent, in the sense that we compare the expectations of DE models with respect to those of the concordance cosmology using the same mass function model, we plan to investigate in a forthcoming paper how sensitive are our observational predictions to the different mass functions fitting formulas.

VII. CONCLUDING REMARKS

In this paper, we have investigated the cluster abundances beyond the conventional ΛCDM cosmology by using several parametrizations for the dark energy. In order to do that, we first performed a joint likelihood analysis using the most recent high quality cosmological data (SNe Ia, CMB shift parameter, and BAOs), thereby obtaining tight constraints on the main cosmological and dark energy free parameters. At the level of the resulting Hubble function, we have found that of all dark energy models (apart from a braneworld cosmology), are statistically indistinguishable (within 1σ) from a flat ΛCDM model, as long as they are confronted with the quoted set of observations.

On the other hand, despite the fact that these models closely reproduce the ΛCDM Hubble expansion, we show that eight out of the 12 studied DE models, using the observationally fitted model parameters, can be differentiated from the reference ΛCDM model on the basis of their redshift distribution of cluster-size halos. Such a comparison was made possible by using the expectations of a future X-ray (based on the eROSITA satellite) and SZ cluster surveys (based on the South Pole Telescope).

The main comparison results can be summarized in the following statements (for nomenclature, see Sec. IV):

(i) Four DE models, namely, XCDM, HRDE, TCM, and PNGB cannot be distinguished from the ΛCDM model at any significant level.

(ii) Seven models, i.e., the BRG, CPL, LRDE, EDE, VCG, Λ_{PS}, and CCDM, can be easily distinguished due to the fact that they show strong and significant variations with respect to the concordance Λ model even at $z = 0$, implying that even with the present-day surveys one could effectively distinguish them.

(iii) The Λ_{RG} model, although it presents relatively small variations with respect to the concordance Λ model, can be clearly distinguished at relatively high redshifts ($z \gtrsim 0.5$).

In a future work we will present a comparison between our model predictions and the observationally determined cluster mass function at different redshifts as well as the available (X-ray or optical) cluster redshift distribution.

[1] A. G. Riess *et al.*, Astrophys. J. **659**, 98 (2007).

[2] W. M. Wood-Vasey *et al.*, Astrophys. J. **666**, 694 (2007); T. M. Davis *et al.*, Astrophys. J. **666**, 716 (2007).

[3] D. N. Spergel *et al.*, Astrophys. J. Suppl. Ser. **170**, 377 (2007).

[4] M. Kowalski *et al.*, Astrophys. J. **686**, 749 (2008).

[5] E. Komatsu *et al.*, Astrophys. J. Suppl. Ser. **180**, 330 (2009); arXiv:1001.4538.

[6] M. Hicken *et al.*, Astrophys. J. **700**, 1097 (2009).

[7] J. A. S. Lima and J. S. Alcaniz, Mon. Not. R. Astron. Soc. **317**, 893 (2000); J. F. Jesus and J. V. Cunha, Astrophys. J. Lett. **690**, L85 (2009).

[8] S. Basilakos and M. Plionis, Astrophys. J. Lett. **714**, L185 (2010).

[9] P. J. Peebles and B. Ratra, Rev. Mod. Phys. **75**, 559 (2003); T. Padmanabhan, Phys. Rep. **380**, 235 (2003); J. A. S. Lima, Braz. J. Phys. **34**, 194 (2004); E. J. Copeland, M. Sami, and S. Tsujikawa, Int. J. Mod. Phys. D **15**, 1753 (2006); M. S. Turner and D. Huterer, Astron. Astrophys. **46**, 385 (2008).

[10] B. Ratra and P. J. E. Peebles, Phys. Rev. D **37**, 3406 (1988).

[11] M. Ozer and O. Taha, Nucl. Phys. **B287**, 776 (1987).

[12] S. Weinberg, Rev. Mod. Phys. **61**, 1 (1989).

[13] W. Chen and Y-S. Wu, Phys. Rev. D **41**, 695 (1990); J. C. Carvalho, J. A. S. Lima, and I. Waga, Phys. Rev. D **46**, 2404 (1992); J. A. S. Lima and J. M. F. Maia, Phys. Rev. D **49**, 5597 (1994); J. A. S. Lima, Phys. Rev. D **54**, 2571 (1996); A. I. Arbab and A. M. M. Abdel-Rahman, Phys. Rev. D **50**, 7725 (1994); J. M. Overduin and F. I. Cooperstock, Phys. Rev. D **58**, 043506 (1998).

[14] S. Basilakos, M. Plionis, and S. Solà, Phys. Rev. D **80**, 083511 (2009).

[15] C. Wetterich, Astron. Astrophys. **301**, 321 (1995).

[16] R. R. Caldwell, R. Dave, and P. J. Steinhardt, Phys. Rev. Lett. **80**, 1582 (1998).

[17] P. Brax and J. Martin, Phys. Lett. B **468**, 40 (1999).

[18] A. Kamenshchik, U. Moschella, and V. Pasquier, Phys. Lett. B **511**, 265 (2001).

[19] A. Feinstein, Phys. Rev. D **66**, 063511 (2002).

[20] R. R. Caldwell, Phys. Lett. B **545**, 23 (2002).

[21] M. C. Bento, O. Bertolami, and A. A. Sen, Phys. Rev. D **70**, 083519 (2004).

[22] L. P. Chimento and A. Feinstein, Mod. Phys. Lett. A **19**, 761 (2004).

[23] E. V. Linder, Phys. Rev. D **70**, 023511 (2004); Rep. Prog. Phys. **71**, 056901 (2008).

[24] A. W. Brookfield, C. van de Bruck, D. F. Mota, and D. Tocchini-Valentini, Phys. Rev. Lett. **96**, 061301 (2006).

[25] J. Grande, J. Solà, and H. Štefančić, J. Cosmol. Astropart. Phys. 08 (2006) 011; Phys. Lett. B **645**, 235 (2007).

[26] C. G. Boehmer and T. Harko, Eur. Phys. J. C **50**, 423 (2007).

[27] J. R. Ellis, N. E. Mavromatos, and D. V. Nanopoulos, Phys. Lett. B **619**, 17 (2005).

[28] A. E. Evrard *et al.*, Astrophys. J. **573**, 7 (2002).

[29] S. Borgani *et al.*, Astrophys. J. **561**, 13 (2001).

[30] T. H. Reiprich and H. Böhringer, Astrophys. J. **567**, 716 (2002).

[31] A. Vikhlinin *et al.*, Astrophys. J. **692**, 1060 (2009).

[32] M. Bartelmann, A. Huss, J. M. Colberg, A. Jenkins, and F. R. Pearce, Astron. Astrophys. **330**, 1 (1998).

[33] H. Dahle, Astrophys. J. **653**, 954 (2006).

[34] V. L. Corless and L. J. King, Mon. Not. R. Astron. Soc. **396**, 315 (2009).

[35] N. A. Bahcall *et al.*, Astrophys. J. **585**, 182 (2003).

[36] Z. L. Wen, J. L. Han, and F. S. Liu, Mon. Not. R. Astron. Soc. **407**, 533 (2010).

[37] J. A. Tauber, in *Proceedings of the 201st Symposium of the International Astronomical Union, Manchester, United Kingdom, 2000* (Astronomical Society of the Pacific, San Francisco, 2005), p. 68.

[38] N. N. Weinberg and M. Kamionkowski, Mon. Not. R. Astron. Soc. **341**, 251 (2003).

[39] L. Liberato and R. Rosenfeld, J. Cosmol. Astropart. Phys. 07 (2006) 009.

[40] M. Manera and D. F. Mota, Mon. Not. R. Astron. Soc. **371**, 1373 (2006).

[41] L. R. Abramo, R. C. Batista, L. Liberato, and R. Rosenfeld, J. Cosmol. Astropart. Phys. 11 (2007) 012.

[42] M. J. Francis, G. F. Lewis, and E. V. Linder, Mon. Not. R. Astron. Soc. **393**, L31 (2009).

[43] M. J. Mortonson, Phys. Rev. D **80**, 123504 (2009).

[44] F. Pace, J-C. Waizmannm, and M. Bartelmann, Mon. Not. R. Astron. Soc. **406**, 1865 (2010).

[45] U. Alam, Z. Lukicánd, and S. Bhattacharya, arXiv:1004.0437.

[46] S. Khedekar and S. Majumdar, arXiv:1005.0388; S. Khedekar, S. Majumdar, and S. Das, Phys. Rev. D **82**, 041301 (2010).

[47] T. D. Saini, S. Raychaudhury, V. Sahni, and A. A. Starobinsky, Phys. Rev. Lett. **85**, 1162 (2000); D. Huterer and M. S. Turner, Phys. Rev. D **64**, 123527 (2001).

[48] E. V. Linder and A. Jenkins, Mon. Not. R. Astron. Soc. **346**, 573 (2003).

[49] D. J. Eisenstein *et al.*, Astrophys. J. **633**, 560 (2005); N. Padmanabhan *et al.*, Mon. Not. R. Astron. Soc. **378**, 852 (2007).

[50] J. R. Bond, G. Efstathiou, and M. Tegmark, Mon. Not. R. Astron. Soc. **291**, L33 (1997).

[51] S. Nesseris and L. Perivolaropoulos, J. Cosmol. Astropart. Phys. 01 (2007) 018.

[52] O. Elgaroy and T. Multamaki, Astron. Astrophys. **471**, 65 (2007); P. S. Corasaniti and A. Melchiorri, Phys. Rev. D **77**, 103507 (2008).

[53] H. Wei, Phys. Lett. B **687**, 286 (2010).

[54] M. Plionis, R. Terlevich, S. Basilakos, F. Bresolin, E. Terlevich, J. Melnick, and R. Chavez, AIP Conf. Proc. **1241**, 267 (2010).

[55] M. Hicken, private communication.

[56] W. Percival *et al.*, Mon. Not. R. Astron. Soc. **401**, 2148 (2010).

[57] M. S. Turner and M. White, Phys. Rev. D **56**, R4439 (1997); T. Chiba, N. Sugiyama, and T. Nakamura, Mon. Not. R. Astron. Soc. **289**, L5 (1997); J. A. S. Lima and J. S. Alcaniz, Astron. Astrophys. **357**, 393 (2000); Astrophys. J. **566**, 15 (2002); J. Kujat, A. M. Linn, R. J. Scherrer, and D. H. Weinberg, Astrophys. J. **572**, 1 (2002).

[58] V. Faraoni, Int. J. Mod. Phys. D **11**, 471 (2002); R. R. Caldwell, M. Kamionkowski, and N. N. Weinberg, Phys. Rev. Lett. **91**, 071301 (2003); J. A. S. Lima and J. S.

Alcaniz, Phys. Lett. B **600**, 191 (2004); G. Izquierdo and D. Pavon, Phys. Lett. B **639**, 1 (2006); S. H. Pereira and J. A. S. Lima, Phys. Lett. B **669**, 266 (2008).

[59] M. Chevallier and D. Polarski, Int. J. Mod. Phys. D **10**, 213 (2001).

[60] E. V. Linder, Phys. Rev. Lett. **90**, 091301 (2003).

[61] C. Deffayet, G. Dvali, and G. Cabadadze, Phys. Rev. D **65**, 044023 (2002).

[62] E. V. Linder and R. N. Cahn, Astropart. Phys. **28**, 481 (2007).

[63] I. Contopoulos and S. Basilakos, Astron. Astrophys. **471**, 59 (2007).

[64] J. A. Frieman, C. T Hill, A. Stebbins, and I. Waga, Phys. Rev. Lett. **75**, 2077 (1995); K. Dutta and L. Sorbo, Phys. Rev. D **75**, 063514 (2007); A. Abrahamse, A. Albrecht, M. Bernard, and B. Bozek, Phys. Rev. D **77**, 103503 (2008).

[65] I. Zlatev, L. Wang, and P. Steinhardt, Phys. Rev. Lett. **82**, 896 (1999); M. Doran, S. Stern, and E. Thommes, J. Cosmol. Astropart. Phys. 04 (2007) 015.

[66] Z. K. Guo and Y. Z. Zhang, Phys. Lett. B **645**, 326 (2007).

[67] M. Makler, S. Q. de Oliveira, and I. Waga, Phys. Lett. B **555**, 1 (2003); M. C. Bento, O. Bertolami, and A. A. Sen, Phys. Lett. B **575**, 172 (2003); A. Dev, J. S. Alcaniz, and D. Jain, Phys. Rev. D **67**, 023515 (2003); Y. Gong and C. K. Duan, Mon. Not. R. Astron. Soc. **352**, 847 (2004); Z. H. Zhu, Astron. Astrophys. **423**, 421 (2004); L. Amendola, I. Waga, and F. Finelli, J. Cosmol. Astropart. Phys. 11 (2005) 009; J. A. S. Lima, J. S. Alcaniz, and J. V. Cunha, Astropart. Phys. **31**, 233 (2009).

[68] I. L. Shapiro and J. Solà, Phys. Lett. B **475**, 236 (2000).

[69] S. Basilakos, Astron. Astrophys. **508**, 575 (2009).

[70] I. L. Shapiro, J. Solà, C. España-Bonet, and P. Ruiz-Lapuente, Phys. Lett. B **574**, 149 (2003); C. España-Bonet, P. Ruiz-Lapuente, I. L. Shapiro, and J. Solà, J. Cosmol. Astropart. Phys. 02 (2004) 006; I. L. Shapiro and J. Solà, Nucl. Phys. B, Proc. Suppl. **127**, 71 (2004).

[71] J. S. Alcaniz and J. A. S. Lima, Phys. Rev. D **72**, 063516 (2005).

[72] I. Prigogine *et al.*, Gen. Relativ. Gravit. **21**, 767 (1989); M. O. Calvão, J. A. S. Lima, and I. Waga, Phys. Lett. A **162**, 223 (1992); J. A. S. Lima and A. S. M. Germano, Phys. Lett. A **170**, 373 (1992); W. Zimdahl and D. Pavòn, Phys. Lett. A **176**, 57 (1993); R. A. Susmann, Classical Quantum Gravity **11**, 1445 (1994); W. Zimdahl and D. Pavón, Mon. Not. R. Astron. Soc. **266**, 872 (1994); Gen. Relativ. Gravit. **26**, 1259 (1994); J. Gariel and G. Le Denmat, Phys. Lett. A **200**, 11 (1995); J. A. S. Lima, A. S. M. Germano, and L. R. W. Abramo, Phys. Rev. D **53**, 4287 (1996).

[73] J. A. S. Lima, F. E. Silva, and R. C. Santos, Classical Quantum Gravity **25**, 205006 (2008); S. Debnath, A. K. Sanyal, arXiv:1005.3933.

[74] G. Steigman, R. C. Santos, and J. A. S. Lima, J. Cosmol. Astropart. Phys. 06 (2009) 033.

[75] J. A. S. Lima, J. F. Jesus, and F. A. Oliveira, arXiv:0911.5727.

[76] S. Basilakos and J. A. S. Lima, Phys. Rev. D **82**, 023504 (2010).

[77] R. C. Arcuri and I. Waga, Phys. Rev. D **50**, 2928 (1994).

[78] J. A. S. Lima, V. Zanchin, and R. Brandenberger, Mon. Not. R. Astron. Soc. **291**, L1 (1997).

[79] F. H. Stabenau and B. Jain, Phys. Rev. D **74**, 084007 (2006).

[80] P. J. E. Peebles, *Principles of Physical Cosmology* (Princeton University, Princeton, NJ, 1993).

[81] R. Gannouji, B. Moraes, and D. Polarski, J. Cosmol. Astropart. Phys. 02 (2009) 034.

[82] V. Silveira and I. Waga, Phys. Rev. D **50**, 4890 (1994).

[83] L. Wang and J. P. Steinhardt, Astrophys. J. **508**, 483 (1998).

[84] S. Basilakos, Astrophys. J. **590**, 636 (2003).

[85] S. Nesseris and L. Perivolaropoulos, Phys. Rev. D **77**, 023504 (2008).

[86] A. Lue, R. Scoccimarro, and G. Starkman, Phys. Rev. D **69**, 044005 (2004).

[87] R. Gannouji and D. Polarski, J. Cosmol. Astropart. Phys. 05 (2008) 018.

[88] W. H. Press and P. Schechter, Astrophys. J. **187**, 425 (1974).

[89] V. R. Eke, S. Cole, and C. S. Frenk, Mon. Not. R. Astron. Soc. **282**, 263 (1996).

[90] J. M. Bardeen, J. R. Bond, N. Kaiser, and A. S. Szalay, Astrophys. J. **304**, 15 (1986); N. Sugiyama, Astrophys. J. Suppl. Ser. **100**, 281 (1995).

[91] A. Jenkins *et al.*, Mon. Not. R. Astron. Soc. **321**, 372 (2001).

[92] L. Marassi and J. A. S. Lima, Int. J. Mod. Phys. D **13**, 1345 (2004); **16**, 445 (2007).

[93] D. Reed, R. Bower, C. Frenk, A. Jenkins, and T. Theuns, Mon. Not. R. Astron. Soc. **374**, 2 (2007).

[94] F. Schmidt, W. Hu, and M. Lima, Phys. Rev. D **81**, 063005 (2010).

[95] J. Dunkley *et al.*, Astrophys. J. Suppl. Ser. **180**, 306 (2009).

[96] E. Rozo *et al.*, Astrophys. J. **713**, 1207 (2010).

[97] L. Fu *et al.*, Astron. Astrophys. **479**, 9 (2008).

[98] R. W. Pike and M. J. Hudson, Astrophys. J. **635**, 11 (2005); A. Cabré and E. Gaztanaga, Mon. Not. R. Astron. Soc. **393**, 1183 (2009).

[99] R. Watkins, H. A. Feldman, and M. J. Hudson, Mon. Not. R. Astron. Soc. **392**, 743 (2009).

[100] C. Fedeli, L. Moscardini, and S. Matarrese, Mon. Not. R. Astron. Soc. **397**, 1125 (2009).

[101] S. Bhattacharya *et al.*, arXiv:1005.2239.